IEEE Access
Multidisciplinary | Rapid Review | Open Access Journal

Received 27 April 2023, accepted 16 May 2023, date of publication 22 May 2023, date of current version 6 June 2023.

Digital Object Identifier 10.1109/ACCESS.2023.3278280

RESEARCH ARTICLE

Thermal Field Simulation and Analysis of Tulip Contact Based on Virtual Material Method

YONGCONG WU[1,2], HANSHENG CAI[1], YI ZHANG[1], AND SHANGMAO HU[1]
[1]Electric Power Research Institute, CSG, Guangzhou 510663, China
[2]School of Electric Power, South China University of Technology, Guangzhou 510641, China

Corresponding author: Yongcong Wu (362121393@qq.com)

ABSTRACT In order to analyze the temperature distribution of circuit breaker tulip contact, a thermal field simulation model for tulip contact is built combined with the electromagnetic-stress-thermal coupled finite element simulation and virtual material method which models the contact resistance characteristics of tulip contact. The temperature rise characteristic of tulip contacts under rated current conditions and short-circuit conditions is analyzed with the model. Results show that the virtual material method can describe the contraction resistance and additional resistance at the end of the contact finger simultaneously, so as to simulate the partial high temperature of the contact interface. Then, the influence of spring pressure and pressure uniformity on the thermal field of tulip contact is analyzed. Results show that the decrease of spring pressure and the imbalance of contact finger pressure may lead to an increase in the temperature rise of the tulip contact. The proposed method can be used as a reference for the design and the overheating analysis of tulip contact.

INDEX TERMS Electromagnetic-stress-thermal, finite element, tulip contact, thermal field, virtual material method.

I. INTRODUCTION

The tulip contact of the circuit breaker is a common location of thermal defects and faults. The micro-deformation of the shell, the inadequate propulsion of the handcart, and the position deviation of the contact will lead to an increase in contact resistance and the increase in contact temperature rise. When the circuit breaker has a high load rate or is subjected to short-circuit current, it may cause local overheating of the tulip contact, which may develop into an insulation fault in severe cases [1].

The electrical contact between the tulip contact and the static contact involves the coupling effect of electromagnetic, stress, and temperature. With the improvement of computer computing performance and numerical calculation theory, multi-physics numerical calculation provides an effective means for the analysis of the above-mentioned problems. And establishing the contact resistance model is a key link in the numerical simulation of the tulip contact temperature rise. The contact resistance model can simulate some physical phenomena such as interface current contraction, local heating, and electric repulsion. In recent years, a variety of contact resistance models have been proposed. In References [2], the contact resistance was equivalent to the contact thermal resistance by establishing a thin layer of contact interface (conductive bridge). Combined with temperature-fluid coupling simulation, the temperature rise differences between common spring tulip contact and memory alloy spring tulip contact were compared. Reference [4] also analyzed the temperature rise of the overlapping point of the gas-insulated busbar by building a conductive bridge model. Reference [5] simulated the current constriction of contacts by the coupled-area method. In [6], W-M fractal characteristic parameters were used to describe the combination of rough surfaces. The three-dimensional (3D) reconstruction of rough surfaces was carried out by fractal dimension and fractal roughness G, and the contact process of micro bulges was analyzed by electromagnetic-stress-temperature coupling numerical calculation. Among the above methods, the application of the conductive bridge method needs to determine the size of the

The associate editor coordinating the review of this manuscript and approving it for publication was Wen-Sheng Zhao.

conductive bridge according to the actual contact area. However, the actual contact area is often unknown for complex contact structures, and the model requires to be modified frequently in conjunction with the stress field calculation results. The coupling area method can be used to calculate the contraction resistance, but the additional resistance caused by the surface protrusion of the material is ignored [7]. Even though the 3D reconstruction method of rough surfaces can realistically restore the microscopic contact behavior of contacts, it is difficult to apply it to multi-physics simulation of electric devices. It may cost a large number of computing resources to restore each contact. In [8], a contact resistance model based on the virtual material method is presented and the thermal stability of the copper lap joint is analyzed. The model not only describes the contact characteristics of the overlapping part but also makes it possible to solve the electromagnetic field, thermal field, and stress field in the same geometric model by giving the nonlinear elastic modulus. It is not necessary to adjust the node coupling mode of discrete elements according to the interface contact condition, which is suitable for application in the numerical simulation of electrical contact.

In this paper, the virtual material method is further applied to the temperature rise calculation of the tulip contact of the circuit breaker. And the heating characteristics and influencing factors of the tulip contact under rated load and short circuit conditions are analyzed by the electromagnetic-stress-temperature coupling calculation. The research can provide a reference for the design of circuit breaker tulip contact and the analysis of overheating defects.

II. THERMAL FIELD CALCULATION MODEL OF CIRCUIT BREAKER TULIP CONTACT

A. BASIC STRUCTURE OF CIRCUIT BREAKER TULIP CONTACT

This paper takes GC5-1250/12 kV bundled tulip contact as an example for modeling and calculation, whose 3D structure and top view are shown in Fig.1. The rated current of the tulip contact is 1250 A, and the rated short-time withstand current of 4 s is 31.5 kA. The tulip tulip contact is formed by copper and plated with silver to prevent oxidation, which contains 30 contact fingers. In the calculation of the stress field, the effect of the spring has been applied to the contact finger as an equivalent pressure boundary, and the grid plate does not exert force on the contact finger during normal operation. Therefore, the spring and the grid plate are omitted from the model. For the calculation of the current field and thermal field, the conductivity and thermal conductivity of the spring and grid plate are much lower than that of copper, so the above simplification has little effect on current and temperature distribution. In addition, since the groove between the moving contact and the contact finger is described by setting different initial distances D_n in the virtual material method, the moving contact is simplified as a cylinder here.

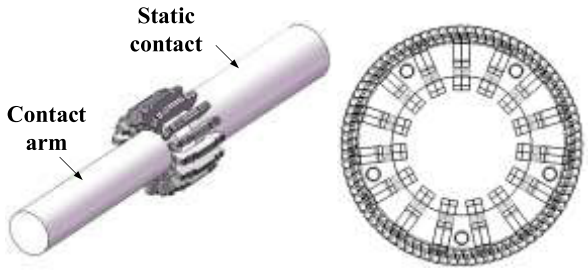

FIGURE 1. Structure of tulip contact.

B. ELECTRICAL CONTACT CALCULATION MODEL OF CONTACT FINGER BASED ON VIRTUAL MATERIAL METHOD

The virtual material method is applied by first creating a thin layer of virtual material that does not actually exist at the contact interface. In contrast to the conductive bridge method, the virtual material method assigns the nonlinear resistivity and elastic modulus to a thin layer, thereby describing both the contact mechanical properties and resistance characteristics of the interface. When the contact surface is partially separated, the equivalent elastic modulus of the virtual material at the separation decreases, so that no negligible additional stress is generated on the metal surface. Thus the interface separation is simulated while ensuring that the model and the node coupling mode remain unchanged. The equivalent resistivity of the virtual material is a function of temperature and pressure, which describes the contact resistance of the interface as a resistance network formed by the non-uniform resistance R_{cn} (n = 1,2,3…) as shown in Fig.2, reflecting the effect of non-uniform stress and temperature. In the electromagnetic-stress-temperature coupling calculation, the resistivity distribution of virtual material is determined by the calculation results of the stress field and thermal field.

The partial model of the contact finger processed by the virtual material is displayed in Fig.2. In reference [8], the equivalent resistivity ρ_{eq} fitting formula of copper material with roughness R_a =0.710 μm was obtained by uniform pressure test and parameter fitting:

$$\rho_{eq}=0.5623P \times (1 + 0.0308 \times (T - 25))/H \qquad (1)$$

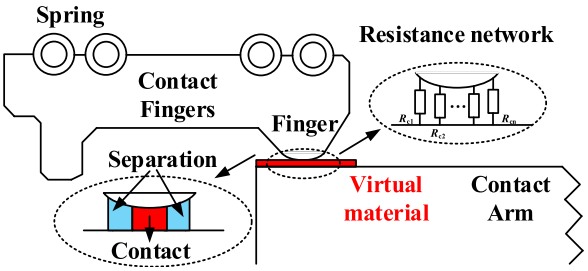

FIGURE 2. Partial model of tulip contact with virtual material.

where ρ_{eq} is the virtual material resistivity ($10^{-8}\Omega$·m); P is compressive stress (Mpa); T is the temperature (°C); H is the virtual material thickness (m).

Since the equivalent resistivity of the virtual material is derived from the resistance network of the interface perpendicular to the current density, in order to make the model meet the above assumptions, according to the current field distribution law at the interface of the medium, the current vector direction and the interface normal direction meet the following conditions:

$$\frac{\tan\alpha_1}{\tan\alpha_2} = \frac{\rho_2}{\rho_1} \tag{2}$$

where ρ_1 and ρ_2 are the resistivity of medium 1 and medium 2 respectively; α_1 and α_2 are the angles between the current vector and the normal direction of the interface in medium 1 and medium 2, respectively.

In order to make the current perpendicular to the interface in the virtual material, the virtual material resistivity ρ_2 should be increased, and combined with (2), it is known that the virtual material thickness should be reduced at this time. Since the incident angle of the current is unknown and different everywhere, the maximum incident angle of the current is estimated to be α_1 =45°. If the maximum incident angle in the current field is larger than 45°, the virtual material parameters should be readjusted. Due to the inability to take the resistivity as infinity in numerical calculations, we take α_2 =2°instead. Comparative simulation proves that the value still meets the accuracy requirements. According to the above parameters, when the medium 1 is copper and the resistivity ρ_{cu} =$1.81\times10^{-8}\Omega$·m, the equivalent resistivity of the virtual material should meet the condition: ρ_{eq} >$28\rho_{cu}$ =$5.07\times10^{-7}\Omega$·m. Together with the calculation results of the stress field below, the results of H <5.8 mm can be obtained by setting P = 0.53 Mpa and T = 25 °C. Therefore, this paper takes H = 5 mm.

As in Fig.3, when the normal displacement of a point on the surface along the plane is greater than the initial value of spacing, the point contacts the plane. In order to ensure the continuous displacement on both sides of the virtual material, the equivalent elastic modulus should be infinite, which is replaced by 1×10^{11} Pa. On the contrary, the contact does not occur when the displacement is less than the initial value. The equivalent elastic modulus should be 0 to eliminate the additional stress on the metal surface. It is taken 1×10^{1} Pa instead in numerical simulation.

The equivalent elastic modulus of the virtual material is shown in (3).

$$E_{eq} = \begin{cases} 1\times10^{11}\text{Pa} & U_n < D_n \\ 1\times10^{1}\text{Pa} & U_n > D_n \end{cases} \tag{3}$$

where U_n is the displacement of each point on the contact surface; D_n is the initial distance between the contact and the target contact surface at the corresponding point.

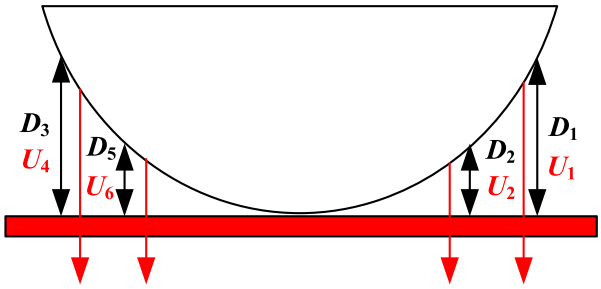

FIGURE 3. Stress distribution of the tulip contact.

C. MULTIPHYSICS COUPLING MODEL

Combined with the virtual material method and the electromagnetic-stress-temperature finite element calculation, the temperature rise characteristics under rated current and short-circuit current of the circuit breaker tulip contact are analyzed.

The stress distribution generated by the spring pressure on the contact finger can be obtained with the steady-state stress field whose control equation are as in (4)∼(7) [9]. As the influence of thermal stress is much less than the stress generated by the spring, thermal stress is ignored to simplify the simulation.

$$(\lambda_m + G)\nabla\theta + G\nabla^2 U + \rho F = 0 \tag{4}$$

$$\theta = \nabla \cdot U \tag{5}$$

$$\lambda_m = \frac{E_m \nu_m}{(1-2\nu_m)(1+\nu_m)} \tag{6}$$

$$G = \frac{E_m}{2(1+\nu_m)} \tag{7}$$

where G is the shear modulus; λ_m is the Lame constant; U is the displacement vector; ν_m is the Poisson's ratio; F is the load vector; Em is the elastic modulus.

Calculated with the spring equivalent pressure as the load, according to the energy balance, the relationship between the total force F_s on the contact piece and the elongation l is [1]:

$$F_s dR = d(\frac{1}{2}kl^2) = kldl \tag{8}$$

where k is the spring rigidity coefficient.

Furthermore, according to the relationship between the spring elongation and the spring radius R, the spring radial force F_s is 2π times the force F_l in the length direction.

$$l = 2\pi\,(R - R_0) \tag{9}$$

$$F_s = 4k\pi^2\,(R - R_0) = 2\pi F_l \tag{10}$$

where R is the actual radius of the spring; R_0 is the initial radius of the spring.

The thermal power of each component is calculated by the eddy current field. And the governing equations of the eddy

current field are as follows [10]:

$$\begin{cases} \nabla \times H = J_e + J_S = J \\ \nabla \times E = -\dfrac{\partial B}{\partial t} \\ \nabla \cdot B = 0 \end{cases} \tag{11}$$

$$\begin{cases} J = \rho_e E \\ B = \mu_e H \end{cases} \tag{12}$$

where H is the magnetic field strength; J_e is vortex current; J_s is the source current; ρ_e is the resistivity; μ_e is the permeability. According to the heat conduction theory, the steady-state form of the thermal field control equation is shown in (13) [11]:

$$k\Delta T + Q = 0 \tag{13}$$

where T is temperature; k is thermal conductivity; Q is the internal heat source.

In the coupling calculation, the total contact area and stress distribution of the virtual material are obtained by stress calculation first. The virtual material resistivity is then determined from the stress distribution and the thermal power distribution of the tulip contact is further analyzed using the eddy current field. Considering that the temperature is related to the resistivity of the virtual material, the resistivity of each point of the virtual material is corrected by the iterative calculation of the thermal field and the eddy current field until the convergence and obtaining the final temperature distribution.

The finite element method is used to solve the electromagnetic-stress-temperature coupling calculation. And the solution process is realized by ANSYS 15.0, which processes the nonlinear parameters by an iterative method. The simulation flowchart and the mesh generation are shown in Fig.4. and Fig.5 respectively. And the total number of elements and nodes are 4084397and 739731, respectively.

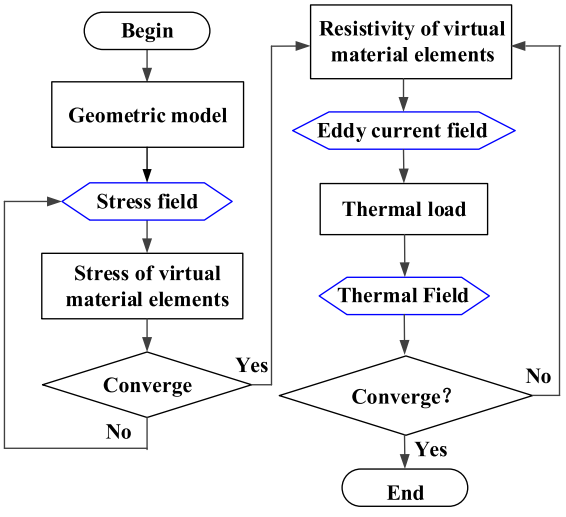

FIGURE 4. Flowchart for thermal field simulation of tulip contact.

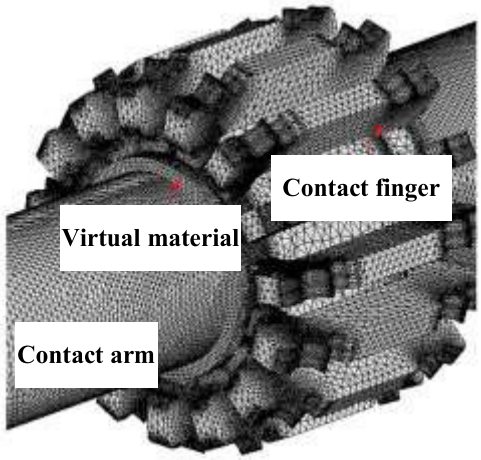

FIGURE 5. Mesh generation of tulip contact.

III. CALCULATION AND ANALYSIS

A. STRESS FIELD CALCULATION RESULTS

The original spring length and the installed spring length are 25 mm and 276 mm respectively. The original length of the spring is 25 mm, and the length of the spring after installation is 276 mm, and the elastic coefficient is 1.4 N/mm. From this, the total force of a single spring on the contact finger is 352 N, which is converted into the equivalent pressure on the pressure surface of the contact finger. The stress distribution of the tulip contact is shown in Fig.6, in which the negative value indicates the compressive stress and the positive value indicates the tensile stress. The calculation results show that the stress concentration area appears at the end of each contact finger, and the maximum compressive stress on the static contact side is 0.53 Mpa. From the stress state of the virtual material, the total contact area between the contact finger and the static contact is 102 mm^2, and the contact area of the single contact finger is 3.4 mm^2. Due to the small curvature radius of the contact finger, the contact area between the contact finger and the static contact is also small.

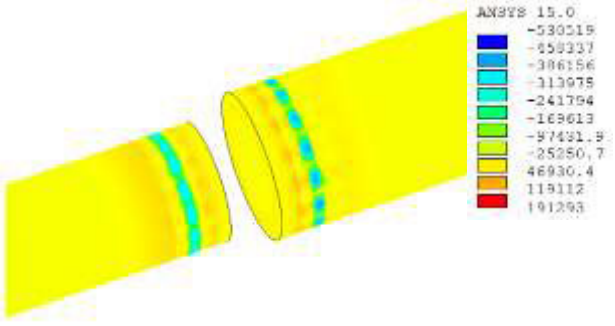

FIGURE 6. Stress distribution of the tulip contact (Pa).

Further observing the displacement distribution of the contact finger in Fig.7, it is found that the maximum deformation

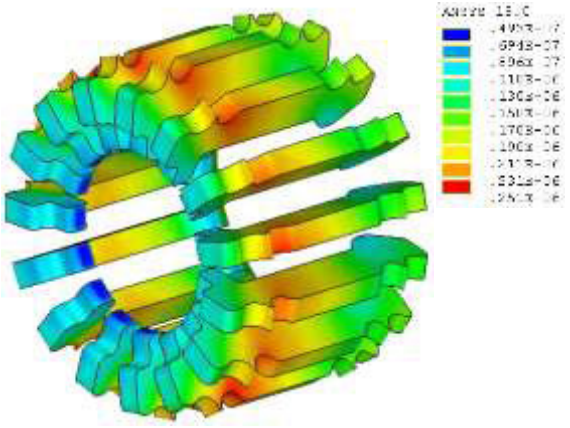

FIGURE 7. Displacement distribution of the contact finger (m).

of the contact finger under the action of spring pressure is 0.25μm.

B. EDDY CURRENT FIELD CALCULATION RESULTS

The current density distribution under the rated current of 1250 A in tulip contact obtained with the eddy current field is shown in Fig.8.

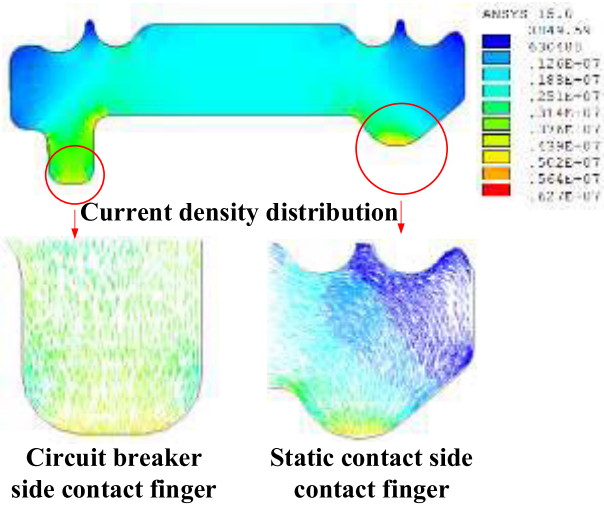

FIGURE 8. Current density distribution of the contact finger (m/A2).

According to the current vector, the maximum incident angle at the interface is less than 45°, which indicates that the above-mentioned hypothesis is reasonable. The calculation results show that the current density shrinks obviously at the contact finger end, and the maximum current density reaches 6.27×10^7 A/m^2, which is greater than the current density of 1.88×10^7 A/m^2 at the contact finger end.

Fig.9 compares the heat generation rate distribution calculated by the coupling area method and the virtual material method. The results manifest that the heat generation rate at the end of the contact finger calculated by the virtual material method reaches 2.46×10^5 W/m^3, whereas the heat generation rate calculated by the coupling area method is only 8.20×10^4 W/m^3. It can be seen that the additional resistance formed by the microscopic bulge of the contact surface is much larger than the contraction resistance formed by the current con-traction. The influence of contraction resistance and additional resistance should be considered simultaneously in the calculation of thermal field.

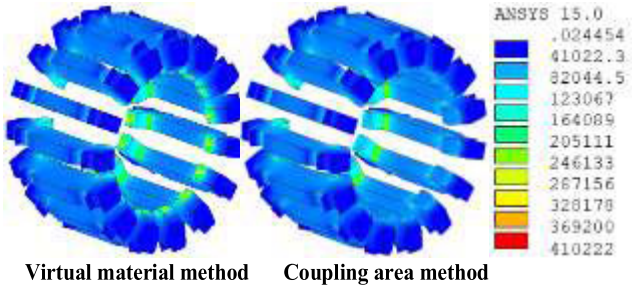

FIGURE 9. Heat generation under different contact resistance (W/m3).

C. THERMAL FIELD CALCULATION RESULTS

1) THERMAL FIELD UNDER 1250 A RATED CURRENT

Taking the heat generation rate obtained with the eddy current field as the heat load, the temperature distribution of the tulip contact under the 1250 A rated current is shown in Fig.10. The convective heat transfer coefficient at tulip contact surface is taken 10 W/(m^2·°C) [12], and the initial temperature and ambient temperature are both 25 °C. Results show that the temperature difference between the contact finger and the contact body is small under steady state in which the heat transfer is fully developed. Besides, the temperature of the contact finger ends on the static contact side is slightly lower than that on the circuit breaker side. Because the equivalent section of the current flow at the contact finger on the circuit breaker side is slightly smaller according to the current path.

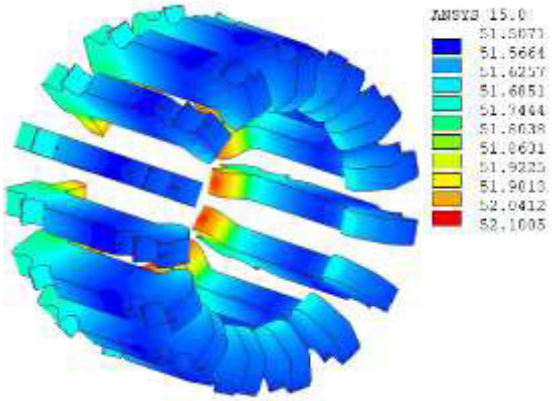

FIGURE 10. Thermal field under rated current 1250A(°C).

2) THERMAL FIELD UNDER 30 KA/4 S SHORT-CIRCUIT CURRENT

When the short-circuit current of 30 kA/4 s is taken into consideration, the final temperature distribution of the tulip

contact after short circuit is shown in Fig 11. Results show that the temperature difference between the contact finger ends and the tulip contact body increases significantly. The maximum temperature of the static contact side and the circuit breaker side are 225.2 °C and 257.5 °C respectively, which are much higher than 96.0 °C of the body. The local overheat suffered by the contact finger end may significant damage and affect the contact performance of the contact fingers. Fig.12. further shows the temperature rise process of the contact finger end and the tulip contact body.

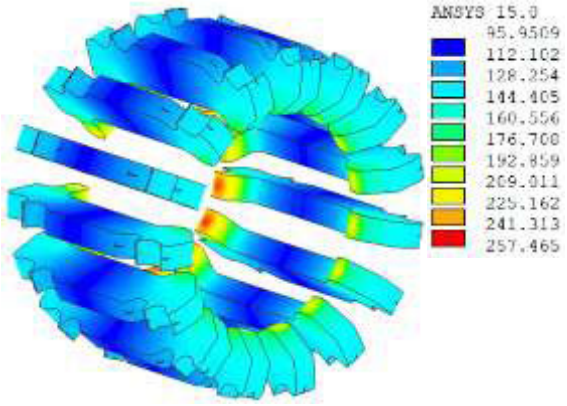

FIGURE 11. Thermal field under short-circuit current 30kA/4s(°C).

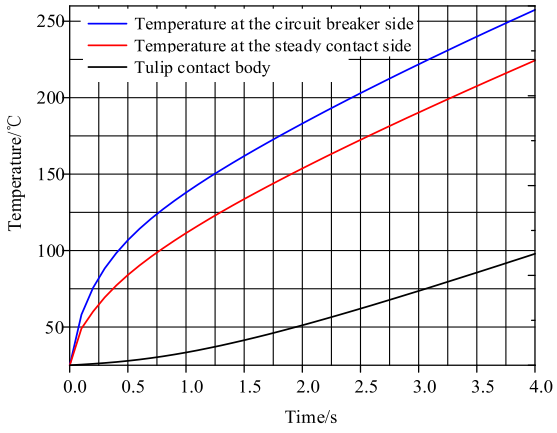

FIGURE 12. Short-circuit temperature rise process(°C).

IV. THE FACTORS INFLUENCING THE TEMPERATURE RISE OF TULIP CONTACT

In practical engineering, the fatigue and failure of tulip contact springs are main reasons for the increase of contact resistance and the formation of overheating. Therefore, the effect of spring pressure variation on the temperature rise of tulip contact is further analyzed.

A. SPRING PRESSURE

Applying different pressure on the equivalent pressure surface of the tulip contact, the relationship between the maximum temperature of the tulip contact and the spring pressure can be obtained under the rated current and 30 kA/4 s short circuit condition, as shown in Fig.13. When the total pressure of the spring is reduced from 352 N to 150 N, the maximum temperature under the rated current condition and that under short circuit condition increases 33 °C and 160 °C respectively. Therefore, ensuring sufficient pressure on the tulip contact spring is the primary factor to reduce the contact resistance and reduce the temperature rise.

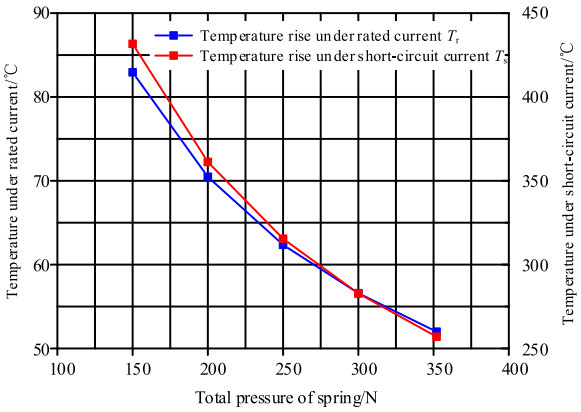

FIGURE 13. Relationship between temperature and spring pressure.

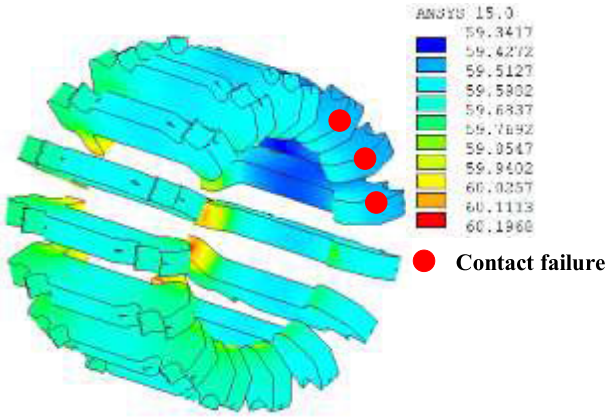

FIGURE 14. Thermal field under rated current 1250A(°C) Contact.

B. THE UNIFORMITY OF CONTACT FINGER PRESSURE

When the handcart is not in place, it may cause the pressure distribution of the contact finger to the static contact to be uneven. The total pressure of the spring is kept at 352 N, and some of the contact fingers acting as pressure load are removed, as shown in FIGURE 14. and FIGURE 15. The spring pressure is uniformly loaded on the remaining contacts to simulate the uneven pressure of the contacts caused by the misalignment of the static contacts.

When the pressure load is not uniform, the contact resistance of the tulip contact increases from 26.7 $\mu\Omega$ to 42.44 $\mu\Omega$. The temperature distribution of the contact under the rated current of 1250 A and the short-circuit current of 30 kA/4 s is shown in Fig.14 and Fig.15, respectively. The

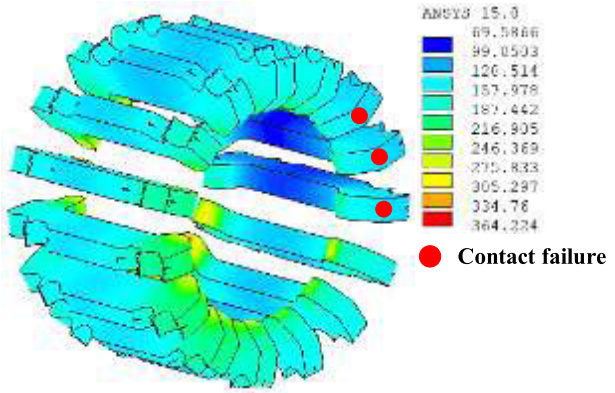

FIGURE 15. Thermal field under short-circuit current 30kA/4s(°C).

maximum steady-state temperature of tulip contact increased from 52.1 °C to 60.20 °C, and the maximum short-circuit temperature increased from 257.5 °C to 364.2 °C. It can be seen that the uneven stress distribution of the contact will also lead to an increase in the overall contact resistance of the tulip contact and an increase in temperature rise. Therefore, the operation personnel should ensure that the circuit breaker handcart is in place to guarantee good contact between each contact finger and the contact.

V. CONCLUSION

In this paper, the thermal field calculation model of tulip contact is established by combining the virtual material method with the electromagnetic-stress-temperature finite element coupling calculation. The virtual material method can simultaneously simulate the contraction resistance and additional resistance of the interface under different external loads, which fully reflects the temperature rise characteristics of the interface under different working conditions. Using the above model, the temperature distribution of tulip contacts under rated current and short-circuit current conditions is obtained, and the influence of spring pressure and contact finger pressure uniformity on the temperature rise of tulip contacts is further analyzed. The method proposed in this paper can provide a valuable reference for the thermal field calculation and design of electrical equipment components.

REFERENCES

[1] M. Huang and L. Chen, "Overheating fault mechanism analysis on circuit breaker handcart contact with measure to prevent," *High Volt. Appar.*, vol. 55, no. 1, pp. 243–248, Jan. 2019.
[2] M. Huang and L. Chen, "Temperature field simulation analysis of breaker tulip contact with memory alloy springs," *J. Electr. Power Sci. Technol.*, vol. 31, no. 3, pp. 146–151, Sep. 2016.
[3] M. Huang, "Simulation on 12 kV 1250A switch tulip contact with memory alloy gaskets," Ph.D. dissertation, School Elect. Eng. Automat., Xiamen Univ. Technol., Xiamen, China, 2016.
[4] X. W. Wu, N. Q. Shu, H. T. Li, and L. Li, "Contact temperature prediction in three-phase gas-insulated bus bars with the finite-element method," *IEEE Trans. Magn.*, vol. 50, no. 2, pp. 277–280, Feb. 2014.
[5] C. Niu, R. Qiang, X. Wang, M. Rong, and G. Jin, "Simulation of high-voltage circuit breaker contact resistance via contact area coupling method," *High Volt. Appar.*, vol. 51, no. 2, pp. 18–23, Feb. 2015.
[6] L. Zhou, T. Lu, B. Zhang, G. Yu, and J. Wan, "Multiphysics coupling analysis of rough surfaces using 3D fractal model," *Trans. China Electrotechnical Soc.*, vol. 30, no. 14, pp. 226–232, Jul. 2015.
[7] G. Wu, Z. Zhou, and C. Tu, "Research on contact resistance of high voltage circuit breaker," *Electric Power Autom. Equip.*, vol. 24, no. 6, pp. 80–82, Dec. 2011.
[8] Y. Wu, J. Ruan, Y. Gong, M. Long, and P. Li, "Contact resistance model and thermal stability analysis of bolt structure," *IEEE Trans. Compon., Packag., Manuf. Technol.*, vol. 9, no. 4, pp. 694–701, Apr. 2019.
[9] X. Guan, N. Shu, B. Kang, and M. Zou, "Multiphysics analysis of plug-in connector under steady and short circuit conditions," *IEEE Trans. Compon., Packag., Manuf. Technol.*, vol. 5, no. 3, pp. 320–327, Mar. 2015.
[10] C. Liao, J. Ruan, C. Liu, W. Wen, S. Wang, and S. Liang, "Comprehensive analysis of 3-D electromagnetic-fluid-thermal fields of oil-immersed transformer," *Electr. Power Autom. Equip.*, vol. 35, no. 9, pp. 150–155, 2015.
[11] Y. Hao, Y. Chen, L. Yang, J. Huang, and M. Fu, "Study on simplification and equivalence of 3D simulation model of HVDC submarine cables," *Southern Power Syst. Technol.*, vol. 11, no. 4, pp. 1–6, May 2017.
[12] B. Wang, J. Jiang, L. Zhao, Y. Fan, and S. Duan, "Temperature field simulation of contact heating in high voltage switchgear," *High Volt. Appar.*, vol. 49, no. 12, pp. 42–47, Dec. 2013.

YONGCONG WU was born in Foshan, Guangdong, China, in 1991. He received the B.Sc. degree in electrical engineering and automation and the Ph.D. degree in high voltage and insulation technology from Wuhan University, Wuhan, China, in 2013 and 2020, respectively. He is currently with the State Key Laboratory of HVDC Transmissions Technology, CSG, China. His current research interests include multi-physics simulation and grounding technology in power systems.

HANSHENG CAI was born in Qichun, Hubei, China, in 1963. He received the B.Sc. degree in electrical engineering and automation from Tianjin University, Tianjin, China, in 1983, and the M.S. degree in high voltage and insulation technology from the Wuhan University of Hydraulic and Electrical Engineering, Wuhan, China, in 1989. He is currently a Senior Engineer with the State Key Laboratory of HVDC Transmissions Technology, CSG, China. His current research interests include power system analysis, overvoltage and insulation coordination, lightning protection and grounding technology, and high voltage measure technology in power systems.

YI ZHANG was born in Tianmen, Hubei, China, in 1984. He received the B.Sc. degree in electrical engineering and automation and the Ph.D. degree from Wuhan University, Wuhan, China, in 2006 and 2015, respectively. He is currently with the State Key Laboratory of HVDC Transmissions Technology, CSG, China. His current research interests include lightning protection and grounding technology and high voltage measurement technology in power systems.

SHANGMAO HU received the M.S. and Ph.D. degrees in electrical engineering from Xi'an Jiaotong University, Xi'an, China, in 2008 and 2012, respectively. He is currently with the State Key Laboratory of HVDC Transmissions Technology, CSG, China. His current research interests include the electrode technology of HVDC, overvoltage, and the protection of power systems.